Matematisk-fysiske Meddelelser
udgivet af
Det Kongelige Danske Videnskabernes Selskab
Bind **32,** nr. 5

Mat. Fys. Medd. Dan. Vid. Selsk. **32,** no. 5 (1960)

ON THE ANGULAR DISTRIBUTION OF THE SCATTERED PARTICLES IN COULOMB EXCITATION

BY

JENS BANG

København 1960
i kommission hos Ejnar Munksgaard

CONTENTS

Synopsis

The angular distribution of scattered particles in Coulomb excitation is calculated for the case of electric quadrupole excitation and vanishing energy transfer; numerical values are given for a number of scattering angles and incident energies. Furthermore, an expression for the cross section at a deflection angle equal to zero is derived, valid also for finite energy transfer.

Printed in Denmark
Bianco Lunos Bogtrykkeri A-S

I. Introduction

The detection of the inelastically scattered particles in Coulomb excitation has recently been used in the investigation of low-lying nuclear states.

This method has certain advantages over the one consisting in detection of the subsequently emitted gamma rays or conversion electrons. Particularly, it is profitable in that it gives information about excitation energies and cross sections which does not depend on any knowledge of the decay scheme and the conversion coefficients.

On the other hand, determination of the cross sections by this method requires either measurements at several deflection angles of the scattered particle or knowledge of the theoretical angular distribution. This angular distribution is essentially independent of the nuclear structure and, when the multipole character of the excitation is given, is calculable from electrodynamics alone. In fact, such calculations have been made by ALDER and WINTHER and the result expressed in terms of the function $\frac{df(\vartheta, \eta, \xi)}{d\Omega}$ (ref. 1, II B. 34), where ϑ is the deflection angle of the scattered particle, and η is defined by

$$\eta = \frac{Z_1 Z_2 e^2}{\hbar v}, \tag{1}$$

where Z_1 and Z_2 are the charge numbers of the projectile and the nucleus, and v their relative velocity. ξ is defined by

$$\xi = \eta_i - \eta_f, \tag{2}$$

where the indices i and f refer to the initial and the final state respectively.

In the case of electric dipole excitation, an explicit expression for $\frac{df_{E1}(\vartheta, \eta, \xi)}{d\Omega}$ in terms of hypergeometric functions was found, but for the other excitation types calculations were only made in the limit of $\eta \to \infty$,

where the motion of the projectile can be described by a classical path, and in the limit of $\eta \to 0$, where the Born approximation applies. In the most important case, namely that of electric quadrupole excitation, the total f-function (integrated over ϑ) was also calculated for intermediate η-values. It was found that the classical approximation was good to 5% down to η-values of the order 4. However, the angular distribution of de-excitation γ-rays, expressed in terms of the a-coefficients (ref. 1, II C. 26), showed a considerable deviation from the classical limit, even for rather high values of η (ref. 1, fig. II. 8). Accordingly, it was thought to be questionable whether the classically calculated differential f-functions could be used in the regions of energies and charges where the experiments are actually made, and a further investigation of $\frac{df}{d\Omega}$ for intermediate values of η was considered desirable.

In the present work, $\frac{df_{E2}(\vartheta, \eta, \xi = 0)}{d\Omega}$ has been calculated (by means of an electronic computor) for ten different angles and six different values of η. The case of $\xi = 0$ was chosen in order to simplify the calculations. Besides, an exact expression for $\frac{df_{E2}(\vartheta = 0, \eta, \xi)}{d\Omega}$ (in terms of hypergeometric functions) is given.

II. Numerical Calculations of the Angular Distribution

The calculations reported here were made from the non-relativistic expressions II B. 34 and II B. 45 of ref. 1:

$$df_{E\lambda}(\vartheta, \eta, \xi) = \frac{4\, k_i k_f a^{2\lambda-2}}{\lambda^2 (2\lambda+1)^3} \sum_{\mu} |\langle \vec{k}_f | r_p^{-\lambda-1} Y_{\lambda\mu}(\vartheta_p, \Phi_p) | \vec{k}_i \rangle|^2 \, d\Omega \tag{3}$$

with

$$\left.\begin{aligned} \langle \vec{k}_f | r_p^{-\lambda-1} Y_{\lambda\mu}(\vartheta_p, \Phi_p) | \vec{k}_i \rangle &= (4\pi)^{\frac{3}{2}} \sum_{l_i l_f m_i m_f} i^{l_i - l_f} (-1)^{\mu} \exp(i\sigma_i + i\sigma_f) \\ \times [(2l_i+1)(2l_f+1)(2\lambda+1)]^{\frac{1}{2}} &\begin{pmatrix} l_i & l_f & \lambda \\ 0 & 0 & 0 \end{pmatrix} \begin{pmatrix} l_i & l_f & \lambda \\ m_i & -m_f & \mu \end{pmatrix} Y_{l_i, -m_i}(\vec{k}_i)\, Y_{l_f, m_f}(\vec{k}_f)\, M_{l_i, l_f}^{-\lambda-1}. \end{aligned}\right\} \tag{4}$$

Here, a is half the distance of closest approach, $a = \frac{Z_1 Z_2 e^2}{m_0 v_i v_f}$ (the reduced mass of the target nucleus and projectile being m_0). The multipole order of the excitation is λ, the expressions in the long brackets are the Clebsch-

TABLE I

$\frac{df_{E2}(\vartheta)}{d\Omega}$

ϑ \ η	0.5	1.0	1.5	2.0	4.0
0°	0.1580 (−3)	0.1267 (−4)	0.3425 (−4)	0.5857 (−4)	0.2065 (−3)
20°	0.3014 (−1)	0.6867 (−1)	0.9909 (−1)	0.1039	0.1027
40°	0.2781 (−1)	0.5826 (−1)	0.7614 (−1)	0.8455 (−1)	0.9059 (−1)
60°	0.2624 (−1)	0.5362 (−1)	0.6565 (−1)	0.7302 (−1)	0.7698 (−1)
80°	0.2553 (−1)	0.4972 (−1)	0.5985 (−1)	0.6527 (−1)	0.6890 (−1)
100°	0.2512 (−1)	0.4699 (−1)	0.5616 (−1)	0.5988 (−1)	0.6315 (−1)
120°	0.2475 (−1)	0.4531 (−1)	0.5342 (−1)	0.5800 (−1)	0.5965 (−1)
140°	0.2448 (−1)	0.4420 (−1)	0.5164 (−1)	0.5453 (−1)	0.5752 (−1)
160°	0.2432 (−1)	0.4344 (−1)	0.5043 (−1)	0.5321 (−1)	0.5603 (−1)
180°	0.2429 (−1)	0.4304 (−1)	0.4987 (−1)	0.5250 (−1)	0.5522 (−1)

TABLE II

ϑ \ $\lim\left(\frac{df_{E2}(\vartheta)}{d\Omega}\cdot\eta^{-2}\right)_{\eta\to 0}$
0° 0.5585 (−1)
20° 0.2189
40° 0.2220
60° 0.2241
80° 0.2238
100° 0.2231
120° 0.2231
140° 0.2235
160° 0.2232
180° 0.2232

TABLE III

$\eta = \infty$

ϑ	$\frac{df_{E2}(\vartheta)}{d\Omega}$
0°	1.676 (−1)
10°	1.385 (−1)
20°	1.178 (−1)
30°	1.027 (−1)
40°	0.916 (−1)
50°	0.832 (−1)
60°	0.768 (−1)
70°	0.719 (−1)
80°	0.680 (−1)
90°	0.650 (−1)
100°	0.627 (−1)
110°	0.608 (−1)
120°	0.593 (−1)
130°	0.582 (−1)
140°	0.573 (−1)
150°	0.566 (−1)
160°	0.562 (−1)
170°	0.559 (−1)
180°	0.558 (−1)

Gordan coefficients in Wigner's notation (see II A. 1 and II A. 6 of ref. 1), the Y_{em} are the normalized spherical harmonics, the σ's are the Coulomb phase shifts, $\sigma_e = \arg \Gamma(l + 1 + i\eta)$, the M's are the radial matrix elements for Coulomb excitation defined in ref. 1, II B. 46, and the wave vector of the projectile is denoted by $\vec{k}$.

If $\lambda = 2$ and $\xi = 0$ ($\eta_i = \eta_f = \eta$), and if furthermore the direction of $\vec{k}_i$ is used for the z-axis, this expression may be written as

$$\frac{df}{d\Omega} = \frac{4\,\eta^2}{5^3} \sum_{\mu} | \langle \vec{k}_f | r^{-3} Y_{2,\mu} | \vec{k}_i \rangle |^2 \tag{5}$$

with

$$\left.\begin{aligned} &\langle \vec{k}_f | r^{-3} Y_{2\mu} | \vec{k}_i \rangle \\ &= 5^{\frac{1}{2}} (4\pi)^{\frac{1}{2}} \sum_{l_i,\, l_f = l_i - 2,\, l_i,\, l_i + 2} i^{l_i - l_f} (-1)^{\mu} e^{i(\sigma_i + \sigma_f)} (2 l_i + 1)(2 l_f + 1) \begin{pmatrix} l_i & l_f & 2 \\ 0 & 0 & 0 \end{pmatrix} \begin{pmatrix} l_i & l_f & 2 \\ 0 & -\mu & \mu \end{pmatrix} \\ &\times \left(\frac{(l_f - \mu)!}{(l_f + \mu)!} \right)^{\frac{1}{2}} M_{l_i l_f}^{-3} P_{l_f}^{\mu}(\cos\vartheta)\, e^{i\mu\varphi} \end{aligned}\right\} \tag{6}$$

and

$$M_{l,\,l+2}^{-3} = M_{l+2,\,l}^{-3} = (6 \,|\, l + 1 + i\eta \,|\, |\, l + 2 + i\eta \,|)^{-1} \tag{7a}$$

$$M_{l,\,l}^{-3} = (2\,l\,(l + 1)\,(2\,l + 1))^{-1} (2\,l + 1 - \pi\eta + 2\,\eta\, \mathrm{Im}\,(\psi(l + 1 + i\eta))). \tag{7b}$$

Here $P_l^m(\cos\vartheta)$ denotes the associate Legendre polynomials with the usual normalization.

The procedure of the calculation was to perform the summation for $0 \leqslant l_i \leqslant 64$. The phases and matrix elements were evaluated by means of recursion formulae, and so were the Legendre polynomials. A fixed maximum value for l_i was considered convenient for computational reasons, and 64 was chosen to ensure a reasonable accuracy in the regions where experiments were made. The result of the calculations is shown in table I and fig. 1. For $\eta \to 0$ the value of $\dfrac{df(\vartheta,\eta)}{d\Omega}$ tends to zero. Table II shows the function $\lim \left[\eta^{-2} \dfrac{df(\vartheta,\eta)}{d\Omega} \right]_{\eta \to 0}$ calculated in the same way. This function is a step function, having a value for $\vartheta = 0$ equal to $^1/_4$ of its value for $\vartheta \neq 0$ (see below). For comparison, $\dfrac{df(\vartheta, \eta = \infty, \xi)}{d\Omega}$ with $\xi = 0$ calculated by ALDER and WINTHER by the semi-classical method (ref. 1, table II) is shown in table III and fig. 1.

III. Errors Involved in the Calculation

The errors involved in the present calculation are of two kinds: 1) the systematic errors introduced by stopping the summation at $l_{\max} = 64$; 2) the more accidental errors arising from the numerical methods employed.

The errors of the first kind behave quite differently for small and for large deflection angles ϑ. This is due to the fact that the signs of the Legendre polynomials $P_l^m(\cos\vartheta)$ are changed when l is increased by an amount of approximately $\frac{\pi}{\vartheta}$. Thus, for $\vartheta \approx \pi$ the series are alternating apart from the slowly varying phases of the M's and the σ's. The omitted rest is then smaller than the first omitted term, which, compared with the whole series, is of the order of magnitude $(\eta/l_{\max})^2$. A comparison between

$$\frac{df(\vartheta=\pi,\,\eta=4,\,\xi=0)}{d\Omega} \quad \text{and} \quad \frac{df(\vartheta=\pi,\,\eta=\infty,\,\xi=0)}{d\Omega}$$

seems to indicate that the actual error is even smaller.

For small deflection angles, the error may be estimated in another way. The expression

$$M_{l_i,\,l_f}^{-\lambda-1} \approx \frac{k^{\lambda-2}}{4\,\eta^{\lambda}} \frac{2\,\pi}{\Gamma\left(\frac{\lambda+1-\mu}{2}\right)} e^{-(l/\eta+\pi/2)\,\xi}\,\xi^{(\lambda-\mu-1)/2}\,(2\,l/\eta)^{-(\lambda+\mu+1)/2} \tag{8}$$

(ref. 1, II E. 83),
valid for $l_i \gg 1$, shows that, owing to the exponential function in M, terms with $l > \frac{\eta}{\xi}$ contribute but a negligible amount to $\frac{df}{d\Omega}$. A break-off of the summation at $l_{\max} > \frac{\eta}{\xi}$ therefore has a minor influence on the cross sections. Apart from the exponential, the M's and the phases are smoothly varying functions of ξ in the neighbourhood of zero. Thus, a calculation for $\xi = 0$ where the summation over l is stopped at a large $l = l_{\max}$, yields a result that does not differ very much from the cross section for $\xi = \eta/l_{\max}$. The effect of the break-off is then that the differential cross section for small angles calculated here corresponds to the case of $\xi = \frac{\eta}{64}$ rather than to that of $\xi = 0$. By comparison with the classical calculations for $\xi \neq 0$ (cf. ref. 1, table II.8 and fig. II.7) one must thus expect to find that the result of the present calculation is much smaller than the true value of $\frac{df}{d\Omega}$ for $\vartheta < \frac{\eta}{64}$.

The second kind of error arises from the numerical calculating procedure. Since each step in the calculations was made with the relative error 10^{-12}, the accuracy of the result rests mainly on the numerical stability of the recurrence formulae used. The matrix elements M and the phase factors were calculated in a straightforward manner from the formulae, and it is easily seen that a relative error Δ_l in the l^{th} term leads to the same relative error in all subsequent terms, which means that no serious error is introduced in this way.

The error introduced by employment of the recurrence formula for the Legendre functions may be estimated as follows. Let the fractional error of the Legendre function at a certain step, n, be $\Delta_n(x)$, i. e., the exact value $P_n^m(x)$ is replaced by $P_n^m(x)\,(1+\Delta_n(x))$. This may also be written

$$P_n^m(x)\,(1+\Delta_n(x)) = P_n^m(x)\,(1+\Delta_n^P(x)) + Q_n^m(x)\,\Delta_n^Q(x), \tag{9}$$

where the $\Delta_n^P(x)$ and $\Delta_n^Q(x)$ are chosen so that, when the fractional error at the nearest preceding step is $\Delta_{n-1}(x)$, one has

$$P_{n-1}^m(x)\,(1+\Delta_{n-1}(x)) = P_{n-1}^m(x)\,(1+\Delta_n^P(x)) + Q_{n-1}^m(x)\,\Delta_n^Q(x). \tag{9a}$$

Here $Q_n^m(x)$ is an associated Legendre function of the second kind. As such functions obey the same recursion relations as the P's, the computed value at any later step, l, derived from $n-1$ and n, is

$$P_l^m(x)\,(1+\Delta_n^P(x)) + Q_l^m(x)\,\Delta_n^Q(x), \tag{10}$$

which indicates a fractional error

$$\left.\begin{aligned} &\Delta_n^P + \frac{Q_l^m}{P_l^m}\,\Delta_n^Q \\ &= \frac{P_n^m Q_{n-1}^m \Delta_n - P_{n-1}^m Q_n^m \Delta_{n-1} + (Q_l^m/P_l^m)\,(\Delta_{n-1}-\Delta_n)\,P_n^m P_{n-1}^m}{P_n^m Q_{n-1}^m - P_{n-1}^m Q_n^m} \\ &= \Delta_n - (\Delta_n - \Delta_{n-1})\left\{\frac{Q_l^m}{P_l^m}\,P_n^m P_{n-1}^m - P_{n-1}^m Q_n^m\right\} \\ &\quad \times (-1)^m \frac{\Gamma\left(1+\frac{n-m}{2}\right)\Gamma\left(\frac{1+n-m}{2}\right)}{2^{2m+1}\,\Gamma\left(\frac{n+m}{2}\right)\Gamma\left(\frac{1+n+m}{2}\right)}. \end{aligned}\right\} \tag{11}$$

This might lead to large errors at the points where Q_l^m or Q_n^m tend towards infinity or P_l^m towards zero. Christoffel's formula (ref. 5, 3.6 (26))

$$Q_p(x) = Q_0(x)\,P_p(x) - W_{p-1}(x) \tag{12}$$

(W_{p-1} being a polynomial in x) together with corresponding formulae for the associated functions, obtained by differentiation of (12), shows, however, that the singularities of the Q's play no part here.

As for the zeros of P_l^m, the asymptotic formula for large l (ref. 5, 3.5 (5))

$$\left.\begin{aligned} &\Gamma\left(l+\frac{3}{2}\right) P_l^m(\cos\vartheta) = 2^{\frac{1}{2}}\,(\pi\sin\theta)^{-\frac{1}{2}}\,\Gamma(l+m+1) \\ &\times \sum_{s=0}^{\infty} (-1)^s \frac{\left(\frac{1}{2}+m\right)_s \left(\frac{1}{2}-m\right)_s}{s!\,(\sin\vartheta)^s \left(l+\frac{s}{2}\right)_s} \sin\left(\left(l+\frac{1}{2}\right)\vartheta + \left(\frac{m}{2}+\frac{1}{4}\right)\pi + \frac{s}{2}\pi\right) \end{aligned}\right\} \tag{13}$$

may be applied. The method of TRICOMI [6] then leads to the expression

$$\vartheta_r^0 = \frac{r - \frac{m}{2} - \frac{1}{4}}{l+\frac{1}{2}}\,\pi + o\,(l^{-2}) \tag{14}$$

for these zeros (r integer).

The distance of the zeros from any of the points for which calculations are made is of the order of magnitude l^{-1}, and, as the functions vary rapidly near the zeros, the ratio $\dfrac{Q_l^m}{P_l^m}$ is at most of the order of magnitude l. For $m = 0$ it would still seem that (11) could give a relative error of the order of magnitude $n \cdot l(\Delta_n - \Delta_{n-1}) \approx l^2 \Delta_n$ for $n \approx l$. However, the formula

$$\frac{Q_n}{P_n} - \frac{Q_l}{P_l} = \sum_{i=n+1}^{l} \frac{1}{iP_i\,P_{l-i}} \tag{11 a}$$

shows that in this case the error is rather of the order of magnitude $l\,(l-n)$ $(\Delta_n - \Delta_{n-1})$.

As regards the error in the final result caused by Δ_{n-1} and Δ_n it must furthermore be remembered that the coefficients M etc. decrease with increasing l. In conclusion it may be stated that the errors introduced by the employment of the numerical methods are negligible compared with that which is committed by breaking off the summation at $l = 64$.

IV. The Cross Section for Vanishing Deflection Angle

In the preceding section it was shown that the decrease for small ϑ of the $\frac{df(\vartheta)}{d\Omega}$ obtained in this calculation is due to the introduction of a finite $l_{\max}$. As the expansion on associate Legendre polynomials is a Fourier analysis, this effect seems to indicate that the cross section (5) for $\xi = 0$ as

TABLE IV

η	$\frac{df_{E2}}{d\Omega}(\vartheta = 0)$
$^1/_2$	0.171 (−3)
1	0.328 (−5)
$1^1/_2$	0.203 (−7)
2	0.143 (−9)
4	0.252 (−19)

a function of ϑ is a step function at $\vartheta = 0$. This is supported by the fact that the classical cross section is a step function with the value 0 for $\vartheta = 0$ when one defines it by the limiting procedure $\xi \to 0$. Also in the Born-approximation limit the function $\lim\left(\eta^{-2}\frac{df(\vartheta,\eta)}{d\Omega}\right)_{\eta\to 0}$ turns out to be a step function. In this case, the summation in (6) is easily carried out for $\vartheta = 0$, the result being just one fourth of the value for $\vartheta \neq 0$.

It would seem to be of little importance to calculate the true value of $\frac{df(\vartheta,\eta,\xi=0)}{d\Omega}$ for $\vartheta = 0$. However, it is possible to give a closed expression for this function, even in the regions of $\xi \neq 0$, $\eta \neq 0$, where the cross section shows a smooth behaviour in the neighbourhood of $\vartheta = 0$.

Starting from the expression

$$df_{E2} = \frac{4\,k_i\,k_f}{5^3}\,a^2 \sum_{\mu} |\langle \vec{k}_f | r_p^{-3} Y_{2\mu}(\theta_p, \Phi_p) | \vec{k}_i \rangle|^2 \, d\Omega \tag{15}$$

with

$$\left.\begin{aligned} |\vec{k}_i\rangle &= e^{-\frac{\pi}{2}\eta_i}\,\Gamma(1+i\eta_i)\,e^{ik_i r\cos\vartheta}\,\Phi(-i\eta_i, 1; ik_i r(1-\cos\vartheta)) \\ |\vec{k}_f\rangle &= e^{-\frac{\pi}{2}\eta_f}\,\Gamma(1-i\eta_f)\,e^{ik_f r\cos\vartheta}\,\Phi(i\eta_f, 1; -ik_f r(1+\cos\vartheta)) \end{aligned}\right\} \tag{16}$$

(Φ being the confluent hypergeometric function (see ref. 5)), where the common direction of $\vec{k}_i$ and $\vec{k}_f$ is chosen as z-axis (ref. 1, II B, eqs. 34, 40, 41), one arrives, as sketched in the appendix, at the formula

$$\frac{df_{E2}(\vartheta=0,\eta,\xi)}{d\Omega}=\frac{4\eta^2}{5^3}\left|\sqrt{5\pi}\exp(-\pi\eta)\,\Gamma(1+i\eta(1-\delta))\,\Gamma(1+i\eta(1+\delta))\right.$$
$$\times\left(\div\frac{2}{3}+\frac{i\eta}{1-2i\eta}\left\{\div 1+(i\eta(1-\delta^2))^{-1}+\frac{2(i\eta(1-\delta^2))-1}{i\eta(1-\delta^2)}\right.\right.$$
$$\times(-\delta)^{-i\eta(1-\delta)}(\delta)^{-i\eta(1+\delta)}-\delta\left[\frac{\Gamma(1+2i\eta)\,\Gamma(-i\eta(1+\delta))}{2\,\Gamma(1+i\eta(1\div\delta))}\right. \tag{17}$$
$$\times(\div 2\delta(1+\delta)^{-1})^{-2i\eta}((1-\delta)/(1+\delta))^{i\eta(1\div\delta)}$$
$$+(-1)^{i\eta(1+\delta)}(2i\eta(1+\delta))^{-1}(-\delta)^{-2i\eta}\times F\left(-2i\eta,1,1-i\eta(1+\delta);\frac{1+\delta}{2}\right)$$
$$\left.\left.\left.+\delta(1+2i\eta)^{-1}(1+\delta)^{-1}F(1,1+i\eta(1+\delta),2+2i\eta;2\delta(1+\delta)^{-1})\right]\right\}\right)\Bigg|^2,$$

where

$$\eta\equiv\frac{\eta_i+\eta_f}{2}$$

$$\delta\equiv\frac{\xi}{2\eta}=\frac{\eta_f-\eta_i}{\eta_f+\eta_i}$$

and the F's are Gauss' hypergeometric functions. To zeroth order in δ the result is

$$\frac{4\eta^2}{5^3}\left|\sqrt{5\pi}\exp(-\pi\eta)\,(\Gamma(1+i\eta))^2\left(\frac{1+i\eta}{3(1-2i\eta)}\div(-\delta)^{-2i\eta}\right)\right|^2. \tag{18}$$

This expression is at first indeterminate, but one may make it finite by multiplying η by $1+i\varepsilon$ and letting ε tend towards zero.

The results of the calculation of $\dfrac{df(\vartheta=0,\eta,\xi=0)}{d\Omega}$ from (18) are shown in table IV. The deviation of that table from the column with $\vartheta=0$ in table I seems to be due to the errors in the calculation of the latter. In the limit of $\eta\to 0$ there is an ambiguity in the calculation of $\eta^{-2}\dfrac{df(0,0,0)}{d\Omega}$ from (18). If the limit of $\eta\to 0$ is used first, and then $\xi\to 0$, the result is $\dfrac{16\pi}{225}$; if the procedure is reversed, the result becomes $\dfrac{4\pi}{225}$. This seems to reflect the ambiguity in the calculation of $\lim\left(\eta^{-2}\dfrac{df(\vartheta=0)}{d\Omega}\right)_{\text{Born}}$ mentioned above.

V. Concluding Remarks

Since the calculation of nuclear matrix elements of Coulomb excitation from measurements of the scattered particles has hitherto been based on the classical calculations, which have been made for a number of ξ values between 0 and 4, the most important result of the present calculation seems to be the fact that it shows a very good agreement with the classical ones. For $\eta = 4$, the deviation of $\frac{df(\eta = 4, \xi = 0)}{d\Omega}$ from $\frac{df(\eta = \infty, \xi = 0)}{d\Omega}$ is less than 2% in the whole angular region where the present calculations are valid ($\vartheta > 20°$). When η is smaller, $\frac{df(\xi = 0)}{d\Omega}$ lies somewhere between the value from the classical calculations and that from the Born approximation.

In fig. 1 the curves are tentatively continued into the region of small angles in the way suggested by the above discussion. The uncertainties which still exist in the evaluation of the $\frac{df}{d\Omega}$ functions for small ϑ are not very serious, judging by the fact that this is a region where the sources of experimental errors are very considerable, and at the same time a region which contributes but a negligible amount to the total cross section.

Also the calculation of $\frac{df(\vartheta = 0)}{d\Omega}$ shows good agreement with the classical calculation. Furthermore it shows that for $\xi \neq 0$ the cross sections must decrease considerably in the forward direction, even for rather small η values.

At present only one set of measurements of the angular dependence of the Coulomb cross section seems to be available. The experiment concerned was made by Elbek and Bockelman [2], who used 6-MeV protons on gold and detected the scattered particles from excitation of the levels at 545 and 279 keV, at angles 60°, 95°, 110°, and 130° with the incident beam. In these cases $\eta = 5.0$ and $\xi = 0.25$ and 0.12, and thus the classical theory is expected to be quite accurate. The experimental results certainly agree with the theory, but the test is not very critical owing to the rather large experimental uncertainties.

Fig. 1. The calculated values of $\frac{df_{E2}(\vartheta)}{d\Omega}$ plotted as functions of ϑ.

As a consequence of the finite number of angular momenta involved in the calculations, the latter are only valid for angles $\vartheta > \frac{\eta}{64}$ (see section III). In the region of smaller angles the curves are tentatively extrapolated (the dashed part of the lines) in a way suggested by the classical curve ($\eta = \infty$) (also dashed) and the isotropy of the Born-approximation angular distribution ($\eta = 0$).

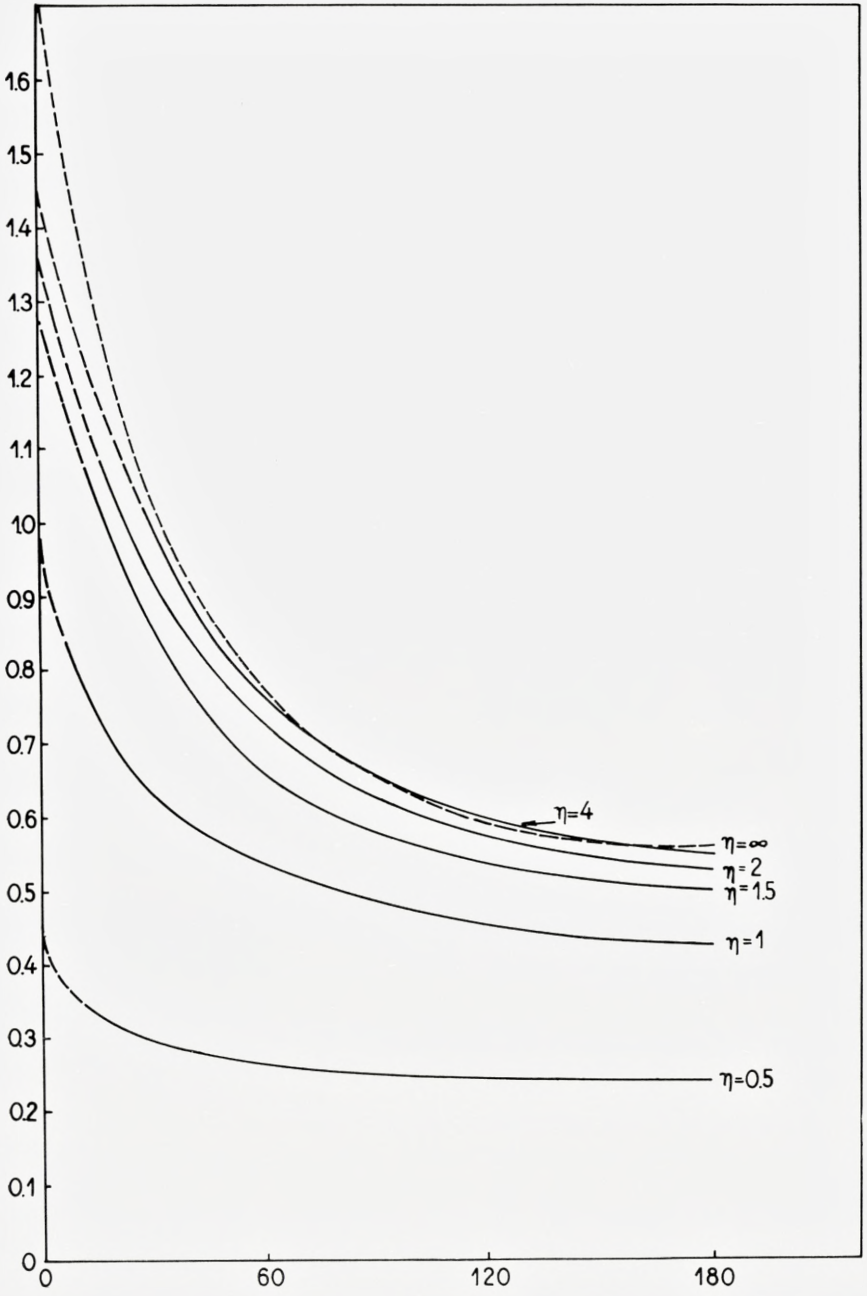
1.6
1.5
1.4
1.3
1.2
1.1
1.0
0.9
0.8
0.7
0.6
0.5
0.4
0.3
0.2
0.1
0
0
60
120
180
η=4
η=∞
η=2
η=1.5
η=1
η=0.5

Acknowledgements

The author wishes to thank Professor Aage Bohr, Dr. S. Rakavy, Per Asisoff, M. Sc., and, particularly, Aage Winther, M. Sc., for valuable suggestions during the present work. Further he wants to express his gratitude to CERN (European Organization for Nuclear Research) and NORDITA for granting him fellowships, and to the board of the Swedish electronic computor BESK for free use of the machine during a period.

NORDITA – Nordisk Institut for Teoretisk Atomfysik
Copenhagen, Denmark

Appendix

The integration in the matrix element (15) may be performed in the following way: the φ-integration is first carried out, leading to 0 for $m \neq 0$ and to 2π for $m = 0$. The wave functions are transformed by means of

$$\Phi(\alpha, \gamma, z) = \exp(z)\, \Phi(\gamma - \alpha, \gamma, -z) \tag{A. 1}$$

(ref. 5, 6.3 (7)) and

$$\Phi(\alpha, 1, z) = \alpha \Phi(\alpha + 1, 2, z) - (\alpha - 1)\, \Phi(\alpha, 2, z) \tag{A. 2}$$

(ref. 5, 6.4 (4)),
and the Y_{20}-function is expressed as a Legendre polynomial $P_2(x)$ $(x = \cos\vartheta)$; the ϑ-integration then becomes

$$\left.\begin{aligned} \mathrm{I} = & -\frac{3}{2}\int_{-1}^{+1} dx\,(1-x)(1+x) \\ & \times [\beta \Phi(\beta+1, 2; -ik_i r(1-x)) - (\beta-1)\, \Phi(\beta, 2; -ik_i r(1-x))] \\ & \times [\beta' \Phi(\beta'+1, 2; -ik_f r(1+x)) - (\beta'-1)\, \Phi(\beta', 2; -ik_f r(1+x))] \\ & + \int_{-1}^{+1} dx\, \Phi(\beta, 1; -ik_i r(1-x))\, \Phi(\beta', 1; -ik_f r(1+x)), \end{aligned}\right\} \tag{A. 3}$$

where $\beta \equiv 1 + i\eta_i$, $\beta' \equiv 1 + i\eta_f$.
This integration may be carried out by means of the theorem

$$\left.\begin{aligned} & \int_0^t \frac{u^{\gamma-1}}{\Gamma(\gamma)}\, \Phi(\beta, \gamma; \lambda u)\, \frac{(t-u)^{\gamma'-1}}{\Gamma(\gamma')}\, \Phi(\beta', \gamma', \lambda'(t-u))\, du \\ & \qquad = \frac{t^{\gamma+\gamma'-1}}{\Gamma(\gamma+\gamma')}\, \Phi_2(\beta, \beta', \gamma+\gamma', \lambda t, \lambda' t), \end{aligned}\right\} \tag{A. 4}$$

which can be proved from ref. 7, 5.4 (9). Here Φ_2 is a confluent hypergeometric function of two variables, defined in 5.7 (21) of ref. 5. By means of the recursion formulae

$$\Phi_2(\gamma+1)\,x = \gamma\,(\Phi_2 - \Phi_2(\beta-1)) \tag{A. 5}$$

and

$$\gamma(\gamma-1)\,\Phi_2(\gamma-1) = \gamma(\gamma-1)\,\Phi_2 + \beta x\,\Phi_2(\gamma+1,\,\beta+1) + \beta' y\,\Phi_2(\gamma+1,\,\beta'+1) \tag{A. 6}$$

the result may be transformed into I =

$$\left.\begin{aligned}
&-\frac{\beta\beta'}{2}\,y,\,\Phi_2(\beta+1,\,\beta'+1,\,5,\,x_1;\,y_1)\\
&+\beta'\left(\frac{\beta}{2}-\frac{1}{3}\right)y_1\,\Phi_2(\beta,\,\beta'+1,\,5;\,x_1,\,y_1)\\
&-\frac{\beta}{3}\,x_1\,\Phi_2(\beta+1,\,\beta',\,5;\,x_1,\,y_1)\\
&+\frac{\beta}{3}\,x_1\,\Phi_2(\beta+1,\,\beta',\,4;\,x_1,\,y_1)\\
&+\frac{\beta'}{3}\,y_1\,\Phi_2(\beta,\,\beta'+1,\,4;\,x_1\,y_1),
\end{aligned}\right\} \tag{A. 7}$$

where $x_1 \equiv -2\,ik_i\,r$, $y_1 \equiv -2\,ik_f\,r$.
If a small imaginary number is added to k_f, the r-integration may be carried out by means of the Laplace integration formula

$$\int_0^\infty dt\,e^{-pt}\,t^{\alpha-1}\,\Phi_2(\beta,\,\beta',\,\gamma,\,xt,\,yt) = \Gamma(\alpha)\,p^{-\alpha}\,F_1\left(\alpha,\,\beta,\,\beta',\,\gamma,\,\frac{x}{p},\,\frac{y}{p}\right)$$

(ref. 7, 4.24 (4)),
where F_1 is a hypergeometric function of two variables, defined in 5.7 (6) of ref. 5.

The result may be contracted considerably by the aid of the recursion formula on pp. 20—21 of ref. 8 and the fact that the variables in the F_1-function become $x = \dfrac{2\,k_i}{k_i+k_f}$ and $y = \dfrac{2\,k_f}{k_i+k_f}$, obeying the relations $x+y=2$,

$$x(\beta-1) = y(\beta'-1) = i\eta\left(1-\left(\frac{\xi}{2\,\eta}\right)^2\right)\left(\eta \equiv \frac{\eta_i+\eta_f}{2}\right).$$

In this way we get

$$\left.\begin{aligned}
\int \mathrm{I}\,e^{i(k_f+k_i)\,r}\,r^{-1}\,dr = -\frac{2}{3} + \frac{i\eta}{1-2\,i\eta}\Bigg\{\left(\frac{\xi}{2\,\eta}\right)^2\Bigg(&F_1(1,\beta,\beta',2;x,y)\\
&+F_1(1,\beta,\beta',1;x,y)\times\frac{1-2x(\beta-1)}{x(\beta-1)}\Bigg)+\frac{1}{ix(\beta-1)}-1\Bigg\}.
\end{aligned}\right\} \tag{A. 8}$$

According to ref. 5, 5.11 (1),

$$F_1(\gamma = 1) = (1-x)^{-\beta}(1-y)^{-\beta'}, \tag{A. 9}$$

whereas, according to the formulae 5.11 (2), 5.11 (10), 5.11 (11), and 5.10 (2) of ref. 5, the function F_1 ($\gamma = 2$) may be expressed as

$$(1-x)^{-1}(-1)^{\beta'}\left\{\frac{(-1)^{-\beta'}}{1-\beta-\beta'}\left(\frac{1-x}{x}\right)F\left(1,\beta',\beta+\beta';\frac{2(x-1)}{x}\right)\right.$$
$$+\frac{1}{\beta'-1}\left(\frac{1-x}{x}\right)^{2-\beta-\beta'}(-2)^{-1}x^{2-\beta-\beta'}F\left(2-\beta-\beta',1,2-\beta';\frac{x}{2}\right)$$
$$\left.+\frac{\Gamma(\beta+\beta'-1)\,\Gamma(1-\beta')}{\Gamma(\beta)}\left(\frac{1-x}{x}\right)^{2-\beta-\beta'}(-2)^{-\beta'}x^{-\beta+1}F\left(1-\beta,\beta',\beta';\frac{x}{2}\right)\right\},$$

where F is the ordinary Gaussian hypergeometric function; here again, according to 2.8 (4) of ref. 5, $F\left(1-\beta,\beta',\beta';\frac{x}{2}\right)=\left(1-\frac{x}{2}\right)^{\beta+1}$, and, to zeroth order in $\left(\frac{\xi}{2\eta}\right)$, $F\left(2-\beta-\beta',1,2-\beta';\frac{x}{2}\right)=\frac{\Gamma(2-\beta)\,\Gamma(\frac{1}{2})}{\Gamma(\frac{3}{2}-\beta)}$ (ref. 5, 2.8 (50)).

This immediately leads to the expression (17)—(18).

References

1) K. Alder, A. Bohr, T. Huus, B. R. Mottelson, and A. Winther, Revs. Mod. Phys. **28** (1956) 432.
2) B. Elbek and C. K. Bockelman, Phys. Rev. **105** (1957) 657.
3) B. Elbek, K. O. Nielsen and M. C. Olesen, Phys. Rev. **108** (1957) 406.
4) V. Ramšak, M. C. Olesen and B. Elbek, Nuclear Physics **6** (1958) 451.
5) A. Erdélyi, W. Magnus, F. Oberhettinger, and F. G. Tricomi, Higher Transcendental Functions (McGraw-Hill, New York, 1953) vol. I.
6) F. G. Tricomi, Ann. Mat. Pura Appl. (4) **26** (1947) 283.
7) A. Erdélyi, W. Magnus, F. Oberhettinger, and F. G. Tricomi, Tables of Integral Transforms (McGraw-Hill, New York, 1954) vol. I.
8) P. Appell and J. Kampé de Fériet, Fonctions Hypergéométriques et Hypersphériques (Gauthiers Villars, Paris, 1926).

Indleveret til selskabet den 24. september 1959.
Færdig fra trykkeriet den 14. maj 1960.